# Rheinische Friedrich-Wilhelms-Universität Bonn

Advanced Laboratory Course

Performed on: May 23 - 24, 2022

Submitted on: June 2x, 2022

---

# E214: ATLAS

---

*Authors*
Keito Watanabe
Paarth Thakkar

*Tutor(s)*
Christina Dimitriadi

**Abstract**

# Contents

# Chapter 1

# Introduction

... This report closely follows the student lab manual from [1]. All the constants for Standard Model (SM) particles were taken from [2].

# Chapter 2

# Theory

## 2.1 The Standard Model

The Standard Model (SM) is one of the most tested theories in physics. It classifies all the known elementary particles into fermions and bosons and describes three of the four known fundamental forces of nature, strong, weak and electromagnetic force [2]. It is a gauge quantum field theory which contains the internal symmetries of the product group, $SU(3) \times SU(2) \times U(1)$. The fermions are spin-1/2 particles and are further classified into quarks and leptons, each with three generations. The bosons are categorized by their spin with gluons, photons, $Z^0$ and $W^{\pm}$ boson having spin 1 and the higgs boson with spin 0. Apart from the gluons and photons, the other bosons are massive. The elementary particles of the SM are shown in Fig. 2.1.1.
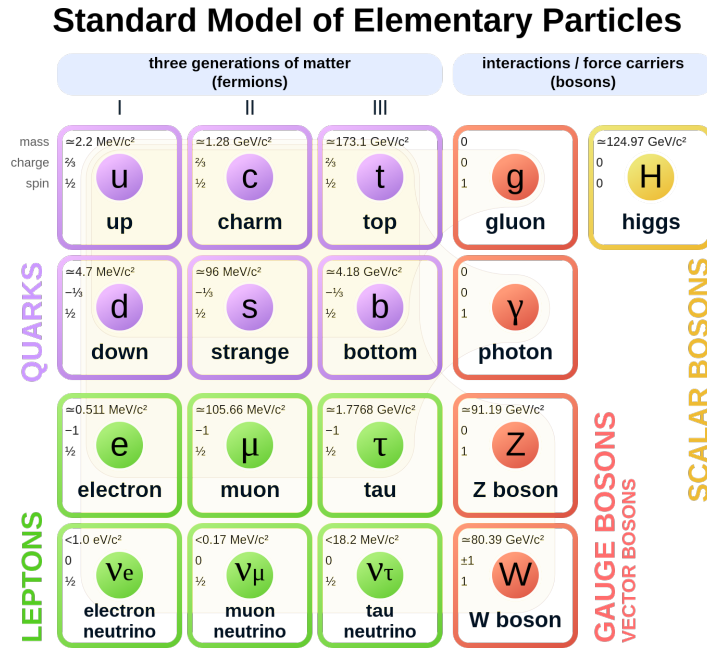


Figure 2.1.1: The Standard Model particles [3].

Despite its huge success, the SM fails at several fronts. It fails to explain matter-antimatter discrepancy, neutrino oscillations, dark matter and hierarchy problem to name a few. In order to test the SM and build a better theoretical framework that tries to answer all of the issues with SM, the Large Hadron Collider (LHC) was built between 1998 and 2008.

## 2.2 LHC and the ATLAS Experiment

## 2.3 The Heavy Gauge Bosons

The $W^{\pm}$ and $Z^0$ are massive bosons which are responsible for the weak forces. The electromagnetic and the weak interactions are unified in the SM to give the electroweak force. The electromagnetic force arises due to $U(1)_Y$ ($Y$ is hypercharge) gauge symmetry and the weak force arises due to $SU(2)_L$ gauge symmetry. After Spontaneous Symmetry Breaking (SSB), the $W^{\pm}$ and $Z$ gain mass while the photon continues to be massless. In this experiment, our aim to is learn the methods of measuring the mass of the $W$ boson. Some important vertices of weak interaction are shown in Fig. 2.3.1.
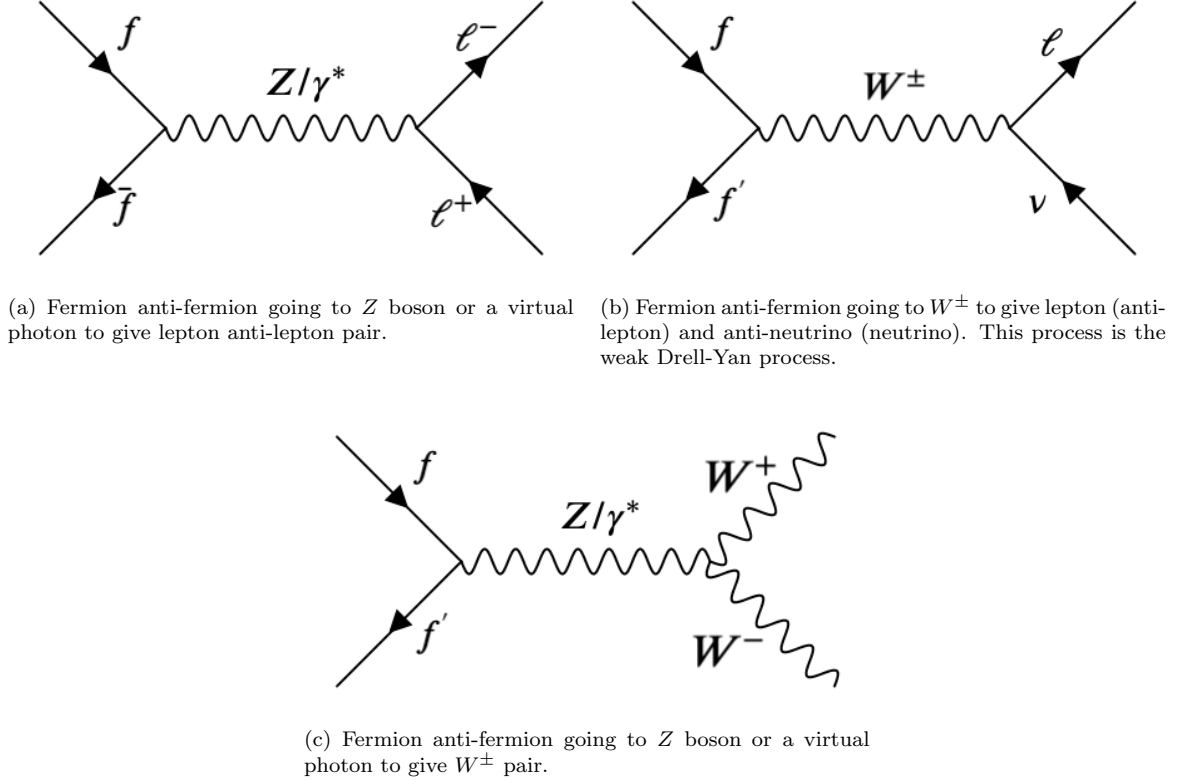


(a) Fermion anti-fermion going to $Z$ boson or a virtual photon to give lepton anti-lepton pair.

(b) Fermion anti-fermion going to $W^{\pm}$ to give lepton (anti-lepton) and anti-neutrino (neutrino). This process is the weak Drell-Yan process.

(c) Fermion anti-fermion going to $Z$ boson or a virtual photon to give $W^{\pm}$ pair.

Figure 2.3.1: Important weak interactions at LHC. Here $f$ stands for fermion and $l$ for leptons.

The mass of the $Z$ boson has been measured with high precision at the LEP accelerator in the year 2006 [4]. Its mass was found to be $91.1876 \pm 0.0021 \, \mathrm{GeV}/c^2$. Since the $Z$ boson decay to leptons (as shown in Fig. 2.3.1a) gives the cleanest signal to reconstruct its invariant mass, these events are usually studied. However, in the case of $W$ boson, which decay to $W \rightarrow e\nu_e$ or $W \rightarrow \mu\nu_\mu$, the invariant cannot be reconstructed directly. This is because neutrinos interact very weakly and are not detected. This makes measuring the mass of the $W$ boson a challenge and it is also one of the less known parameters of the SM. As of writing this report, a high precision measurement by the CDF collaboration of $W$ boson mass was made in April, giving a value of $80.433 \pm 0.009 \, \mathrm{GeV}/c^2$ [5]. This result has a $7\sigma$ deviation from the SM prediction, suggesting inaccuracies in the calculations or possibility of new physics. Before this, the most precise measurement was made in 2018 and found to be $80.379 \pm 0.012 \, \mathrm{GeV}/c^2$ [6].

There are two notable ways to measure the mass of the $W$ boson. The first utilizes the variable $\mathrm{M_T}$, which is defined as

$$\mathrm{M_T} = \sqrt{2p_{T_e} p_{T_\nu}(1 - \cos(\phi_e - \phi_\nu))}, \tag{2.3.1}$$

where $p_{T_e}$ and $p_{T_\nu}$ are the transverse momentum of the electron and neutrino respectively, $\phi_e$ and $\phi_\nu$ are the azimuthal angles. If we consider the mass of the electron to be zero, $\mathrm{M_T}$ is equal to W mass. The distribution of $\mathrm{M_T}$ gives us a Jacobi peak at the W mass. The advantage of using this method is that the transverse of momentum of the $W$ boson does not significantly affect the position of the peak.

The disadvantage is the use of $p_{T_\nu}$, which as mentioned before, cannot be measured directly. Hence, it must be approximated using $\not{E}_T$, which is missing transverse momentum, given by

$$\vec{\not{E}}_T = -\sum_i E^i \sin\theta_i \vec{n}_{i,\perp}, \tag{2.3.2}$$

where $E^i$ is the energy of the $i$-th entry in the calorimeter, $\theta_i$ is the polar angle of the entry and $\vec{n}_{i,\perp}$ is the unit vector pointing towards energy entry in the x-y plane. Which means, that in order to measure $M_T$ accurately, $\not{E}_T$ has to be well calibrated.

The second method to measure the $W$ mass is by studying the transverse momentum spectrum of the leptons using

$$\frac{d\sigma}{dp_T} = \frac{d\sigma}{d\cos\theta^*}\left|\frac{dp_T}{d\cos\theta^*}\right|^{-1} = \frac{d\sigma}{d\cos\theta^*}\frac{2p_T}{M_W}\frac{1}{\sqrt{1/4\ M_W^2 - p_T^2}}. \tag{2.3.3}$$

This gives a Jacobi peak as shown in Fig. 2.3.2. The peak is at half of $W$ mass, therefore, one can measure this peak in order to deduce the $W$ mass. However, the figure shows the ideal case, in which the $W$ boson does not have an initial transverse momentum. As shown in the same figure, if $W$ has an initial momentum, there is a spread in the distribution and a shift in the Jacobi peak. Other factors that can increase the spread are the resolution of the detector and $W$-decay width. However, the advantage of using this method is that it does not require the complicated calibration of $\not{E}_T$. In this experiment we use this method. An interesting side note, the recent high precision measurement from 2022 used the first method to measure the $W$ mass [5].
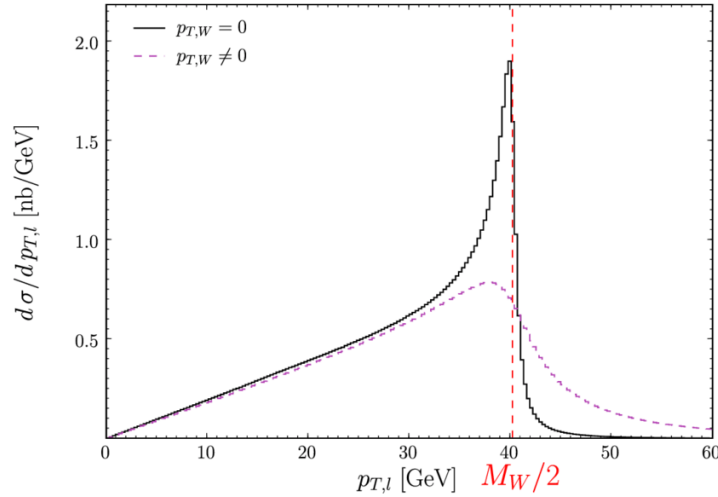


Figure 2.3.2: $p_T$ spectrum of leptons from the $W \to l\nu$ decay. We see a Jacobi peak at half the mass of W boson [7].

# Chapter 3

# Pre-lab Questions

## 3.1 Part 2: Calibration of Electrons

1. Which value does the momentum of an electron have in the decay of a $Z^0$ boson $Z^0 \rightarrow e^+ + e^-$, if the $Z^0$ is at rest?

Solution:
Given that the $Z^0$ boson is at rest, $\vec{p}_Z = 0 \implies E_Z^2 = \vec{p}_Z^2 + m_Z^2 = m_Z^2$ so that $E_Z = m_Z$. This implies that the 4-momentum of the $Z^0$-boson is $p_Z = (m_Z, \vec{0})$. Now by conservation of 4-momentum, we know that $p_Z = p_{e^+} + p_{e^-} \implies p_{e^+} = p_Z - p_{e^-}$.
Now taking the dot product of $p_{e^+}$, we have that:

$$p_{e^+} \cdot p_{e^+} = m_e^2 = (p_Z - p_{e^-}) \cdot (p_Z - p_{e^-}) = m_Z^2 + m_e^2 - 2p_Z \cdot p_{e^-} = m_Z^2 + m_e^2 - 2m_Z E_e$$

$$\implies m_Z = 2E_e => E_e = \frac{m_Z}{2}$$

where the property $(p \cdot p) = E^2 - \vec{p}^2 = m^2$ was used.
To then determine the momentum of the electron, we use the energy-momentum relation again:

$$E_e^2 = \vec{p}_e^2 + m_e^2 \implies |\vec{p}_e| = \sqrt{E_e^2 - m_e^2} = \sqrt{\left(\frac{m_Z}{2}\right)^2 - m_e^2}$$

$$\implies |\vec{p}_e| = \sqrt{\left(\frac{91.18\text{GeV}}{2}\right)^2 - (5.11 \times 10^{-4}\text{GeV})^2} \approx 45.59\text{GeV}$$

where the mass of the electron was neglected.
Thus the momentum of the electron from a $Z^0$ boson decay at rest is $|\vec{p}_e| = 45.59\text{GeV}$.

2. How large is the momentum of tau leptons in the reaction $e^+ + e^- \rightarrow \tau^+ + \tau^-$, if the reaction takes place in the center-of-mass system (center-of-mass energy = 5 GeV)?

Solution:
We know that the mass of the tau lepton is $m_\tau = 1.776$ GeV. Given that the CoM energy is $\sqrt{s} = 5$ GeV, by conservation of energy we have that:

$$s = (2E_e)^2 = (2E_\tau)^2 = 4(\vec{p}_\tau^2 + m_\tau^2) \implies |\vec{p}_\tau| = \sqrt{\frac{s}{4} - m_\tau^2}$$

$$\implies |\vec{p}_\tau| = \sqrt{\frac{(5\text{GeV})^2}{4} - (1.776\text{GeV})^2} = 1.7595\text{GeV}$$

## 3.2 Part 3.1: W-Boson Measurement

1. As before, the analysis is based on ROOT trees. One of the tree variables is `ptw` - the estimated transverse momentum of the W boson candidate. This variable can be constructed from the other tree variables. Please think about how this could be done. The tree variables are listed in section B.

Solution:
Given that the weak interaction is described by $W \rightarrow l + \bar{\nu}_l$, we can calculate the transverse momentum of the W-boson from the transverse momentum of $l$ and $\bar{\nu}_l$. The formula to evaluate this is:

$$p_{T_W} = \sqrt{p_{T_l}^2 + p_{T_\nu}^2}$$

which is derived from the conservation of 3-momentum.
This is defined in ROOT as `el_pt` and `etmis`, so that the transverse momentum of the W boson candidate can be calculated as such: $\sqrt{\texttt{el\_pt}^2 + \texttt{etmis}^2}$.

2. When fitting measurements to a linear function, the two parameters of a best fit straight line are y-intercept and slope. The errors on these parameters are typically correlated. Using these parameters for the error analysis will require a treatment that takes correlations into account. For example the simplest form of Gauss' error propagation law requires that the errors are uncorrelated. Please look up the correct form of the Gauss error propagation law in the presence of correlations. You will need that for the final error on the W mass. On the other hand, is it possible to minimize correlations by choosing an appropriate coordinate system?

Solution:
The Gauss error propagation law in the presence of correlations is given as such:

$$\sigma_f^2 = \left(\frac{df}{dx}\right)^2 \sigma_x^2 + \left(\frac{df}{dy}\right)^2 \sigma_y^2 + 2\left(\frac{df}{dx}\right)\left(\frac{df}{dy}\right)\rho_{xy}\sigma_x\sigma_y$$

where $\rho_{xy}$ is the correlation coefficient which yields zero for uncorrelated errors. The correlation matrix is then defined with the variance $\sigma_x^2, \sigma_y^2$ in its diagonals with the correlations $\rho_{xy}\sigma_x\sigma_y$ in the off-diagonal components.
To minimize correlations, we can convert to an appropriate coordinate system in which the correlation matrix becomes diagonal. This will allow the cross terms to vanish.

## 3.3 Part 3.2: New Physics

1. What is the minimum invariant 4-lepton-mass, when the four leptons originate from a $Z^0$ pair? Why do you find 4-lepton-events with invariant mass beneath this threshold?

Solution:
In theory, the minimum invariant mass of the each lepton should be $m_Z/2$. In addition to the lowest order Feynman diagrams, there are two higher order diagrams where the photon is radiated by initial-state quarks, called Initial State Radiation (ISR), due to which there is a shift in the energy of the ingoing particles, leading to a distortion in the shape of the $Z$ resonance curve. Therefore, the effect of ISR is reduce the effective centre-of-mass energy of the ingoing particles, which leads to some fraction of $Z$ boson invariant mass to be beneath this threshold. Another possible reason can be that in the case of more than one Z boson, the other Z boson will not be on-shell due to kinematic reasons. Due to this, we get one Z boson and another virtual Z* boson. Hence, the mass of the 4 leptons, would be below the threshold.

2. Consider a Higgs boson which decays into two $Z^0$ bosons. How does the distribution of the 4-lepton-invariant-mass look like?

Solution:
The distribution will follow a Voigt function peaked at 125 GeV (Fig. 3.3.1).

3. Assume you have an ideal detector. What is the typical $\not{E}_T$ if a $Z^0$ pair has been produced and both $Z^0$ decay into electron or muon pairs? What $\not{E}_T$ will you expect when you have a real detector?

Solution:
In an ideal case, the expected $\not{E}_T$ is 0. In the case of real detector, $\not{E}_T$ will be non-zero due to inefficiencies in the detector and reconstruction algorithms. Further, not all muons and electrons will be detected. Or, one of the leptons could be extremely soft and not be detected at all.
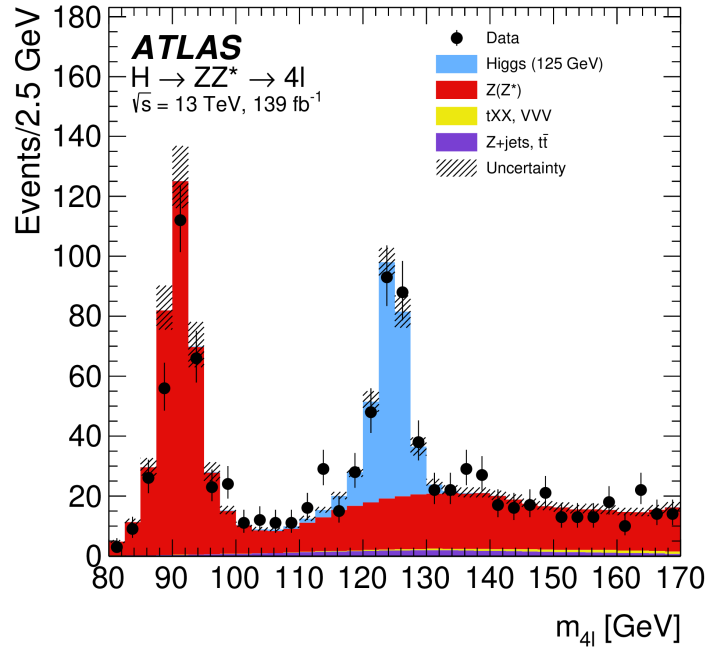
Figure 3.3.1: ATLAS four lepton invariant mass measurement showing evidence for the Higgs boson [8].

4. The Branching ratio of $t \to Wb$ is almost 100%. If you have a top anti-top pair in an event, both particles decay instantly via $t \to Wb$. If both W bosons each decay leptonically $(W \to l\nu)$, one finds two leptons in the event. What could explain the occurence of four leptons in a $t\bar{t}$ event?

Solution:

- One of the leptons radiates a photon/Z* boson which gives lepton-antilepton pair, $l \to l + \gamma \to l + l^{+} + l^{-}$.

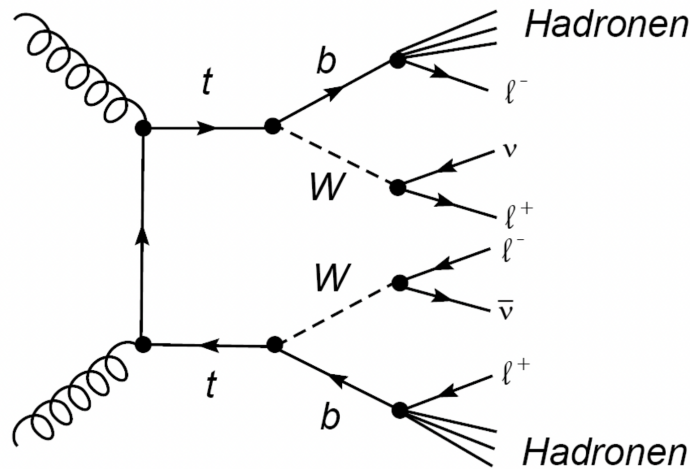- b-quark can decay semi-leptonically, giving us hadrons plus a lepton (Fig. 3.3.2).



Figure 3.3.2: Top and b-quark decay process [1].

# Chapter 4

# Analysis

## 4.1  Part 1: ATLANTIS

In this part of the lab, we get familiar with the program `ATLANTIS`, which displays particle reactions in the ATLAS detector, graphically. ...

Before looking at the assignments for this part, we first become acquainted with all the data sets. We present our observations below.

### 4.1.1  Wenu Data set

In this data set, a $W$ boson decays like, $W^+ \to e^- \bar{\nu}_e$ or $W^+ \to e^+ \nu_e$. This means that the event will contain missing transverse momentum. In Fig. 4.1.1, we see the event 9 from the data set. Starting from the vertex, we see two curved tracks in the top left figure, which deposit their energy in the ECAL. On the opposite side we also notice a huge deposition of hadrons in the HCAL. In the same direction, there is also the line for the $\vec{\not{E}}_T$. In the bottom figure, we see a huge number of deposits in the HCAL.
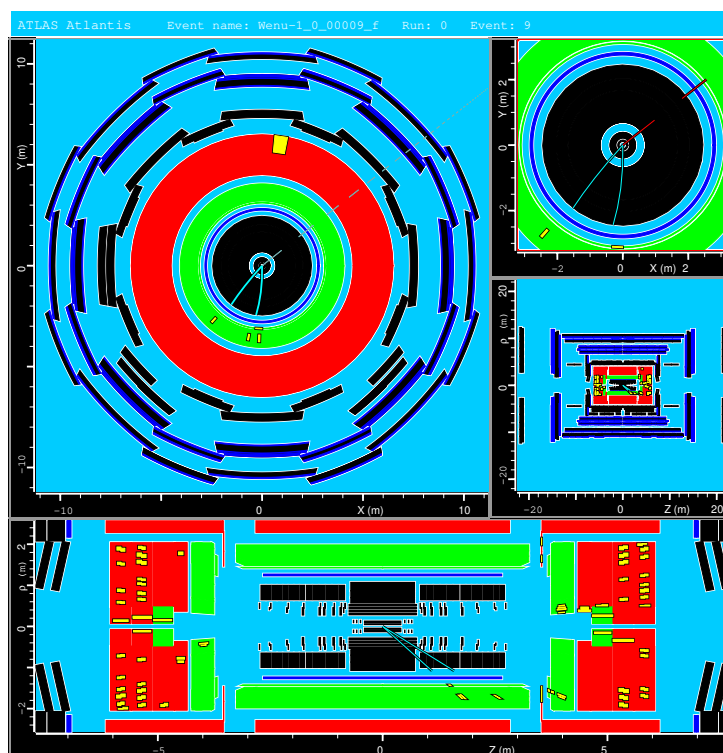


Figure 4.1.1: Event name: `Wenu-1_0_00009_f`, Event: 9.

Since the event contains the decay $W \to e\nu$, one of the tracks which is opposite the $\vec{\not{E}}_T$ vector is

mostly likely the electron from this decay. By using the pick function, we can see the details of $\vec{\not{E}}_T$, which are:

```
ETMis:
 storegate key: MET_Final
 Sum-ET  = 45.688 GeV
 ET-Mis  = 31.907 GeV
 ETx-Mis = 25.086 GeV
 ETy-Mis = 19.716 GeV
 φ = 38.165°
```

The branching ratio (BR) of $W$ boson decay to jets is 67.46% [9]. Because of that we see a huge number of deposits in the HCAL for this event. For comparison, the BR of $W \to e\nu$ decay is 10.83%.

### 4.1.2 WFull Data set

Next, we study the `WFull-1-f.zip` data set. In this, all possible decays of $W$ boson can be seen. In Fig. 4.1.2, starting from the vertex, several curved tracks emerge, indicating the presence of charged leptons and hadrons. Some cures disappear before reaching the ECAL, most likely due to their low momentum (sometimes called "soft" particles). The charged leptons leave their deposit in the ECAL and hadrons in the HCAL. For several deposits, we see an alignment, i.e., the jets contain leptons as well. This could be due to top quark, which decays to $t \to W^+ b$, from which we get jets from the $b$ quark and lepton and neutrino from the $W$.
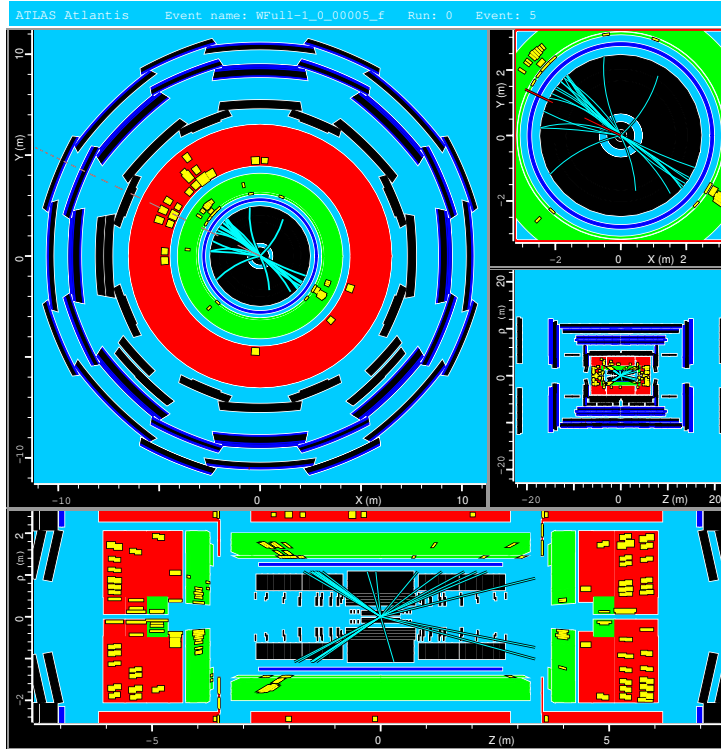


Figure 4.1.2: Event name: `WFull-1_0_00005_f`, Event: 5.

The $\vec{\not{E}}_T$ is found to be

```
ETMis:
 storegate key: MET_Final
 Sum-ET  = 250.750 GeV
 ET-Mis  = 14.408 GeV
 ETx-Mis = -12.976 GeV
```

```
ETy-Mis = 6.263 GeV
φ = 154.236°
```

which is quite high as compared to previous data set, indicating a high number of neutrinos and $W$ boson decays in the event. Further, there is a high number of deposits in the forward sections in the HCAL. This is an expected behavior, since the angular distribution of final state hadrons increases strongly in the forward region [1].

### 4.1.3   Zee Data set

Now we look at the `Zee-1-f.zip` data set. In Fig. 4.1.3, we see the event 3. Similar to our previous discussion, we see several tracks followed by deposits in ECAL and HCAL, with the presence of $\vec{\not{E}}_T$. An interesting feature of this data set is that several ECAL deposits are often opposite to each other. This means that the mother $Z$ boson was most likely at rest when these electrons were produced, giving us this characteristic.
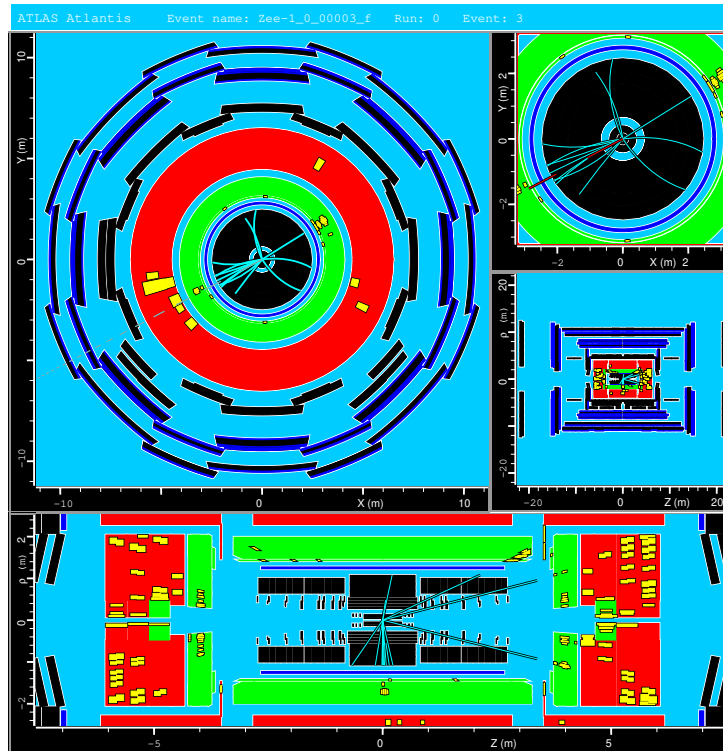


Figure 4.1.3: Event name: `Zee-1_0_00003_f`, Event: 3.

Next, we work with two of the assignments listed in the lab manual. Since we were allowed to pick the assignments on our own, we chose to work with the `mystery-035-f.zip` data set and `ATLASData-Cosmics-M5.zip` data set.

### 4.1.4   Assignment 7: Mystery Data Set

In this data set, a pre-selection is applied, in which at least two leptons ($e$ or $\mu$) are required to be in each event. The goal of this exercise is to look at the graphics and identify various Standard-Model processes by studying them. Further, we must try to rule out certain processes, if any. In Fig. 4.1.4, we see the graphical view of event 13. Fig. 4.1.5, gives us the zoomed in view of the vertex for the same event. We start our discussion from the vertex.

A zoomed in view of the vertex shows that most tracks originate from the vertex, but some a reasonably far away from the vertex. The tracks originating far away from the vertex must come from a particle which has decayed after a certain period of time. This gives us the following three possibilities for the original particle: $\tau^{\pm}$ lepton, top quark or b-quarks (b-jet). Since $W$ and $Z$ boson decay almost immediately, the track reconstruction resolution would not be able to pick on the slight differences in the vertex due to those decays.

As these particles start heading towards the detector, we see that charged particles are bent based on their momentum and leave a "hit" in the inner detector. Some particles are too "soft" and hence their tracks disappear before reaching the ECAL. Looking at the deposition at the ECAL and HCAL, we see that most depositions between them align with each other. This indicates the presence of charged electrons and photons in jets. We know that b-jets contain leptons, as in 25% of all B decays, a lepton is produced. We can get this b-quark from the top quarks via $t \rightarrow W^+ b$. The figure in the bottom half also shows the presence of isolated jets, without leptons. Since $\tau$ leptons can decay purely to hadrons and neutrinos, one of the ways to identify them is to look for collimated "mini" jets.

Two other interesting tracks we see in the ECAL and HCAL are the isolated depositions in ECAL which do not have a corresponding deposition in the HCAL. This means that these charged electrons can come from the following sources: photons, $W$ bosons, $Z$ bosons and $\tau$ leptons. The presence of missing energy in the event confirms the existence of neutrinos and hence, confirms the possibility of $W$ boson decays. The other interesting track corresponds to the deposition in HCAL and then a track in the muon detector. This confirms the presence of muons in the event, which was probably surrounded by jets. Ths could be either due to top quarks or b-quarks.
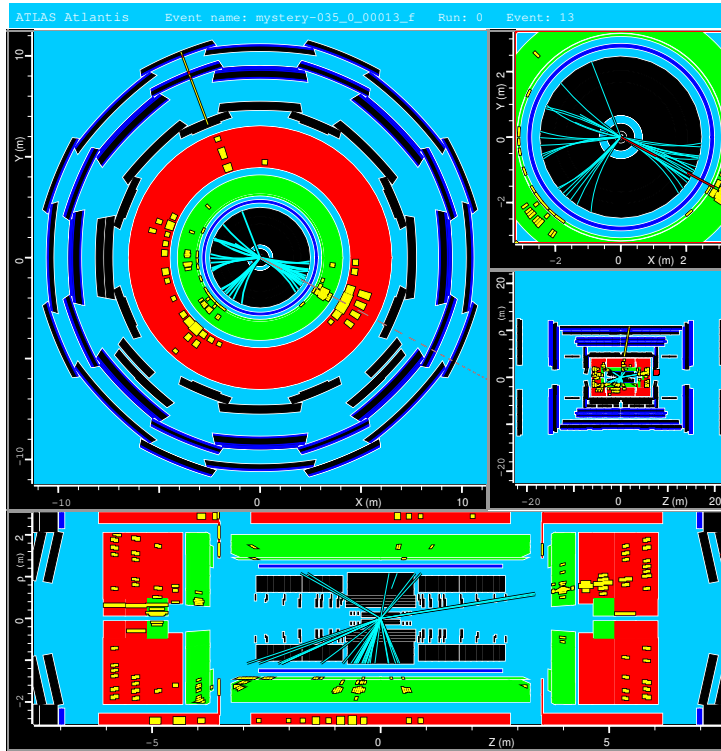


Figure 4.1.4: Event name: `mystery-035-f`, Event: 13.

We look at one more event in Fig. 4.1.6, event 12. In this event as well, we see all of the properties discussed above. Some thing which are slightly different is a higher number of isolated deposits in ECAL (without the corresponding deposit in HCAL) and the presence of two muons instead of a single one, both in the presence of jets. By selecting the missing energy track, we can look at the numbers. The following output was shown in the terminal:

```
ETMis:
 storegate key: MET_Final
 Sum-ET  = 1087.585 GeV
 ET-Mis  = 30.292 GeV
 ETx-Mis = -30.055 GeV
 ETy-Mis = 3.781 GeV
 φ = 172.829°
```

Since the $\not{E}_T$ is quite high, we can confirm the existence of one or more neutrinos in the event. Based on the discussion above, it is not possible to rule out any SM process for two lepton events.
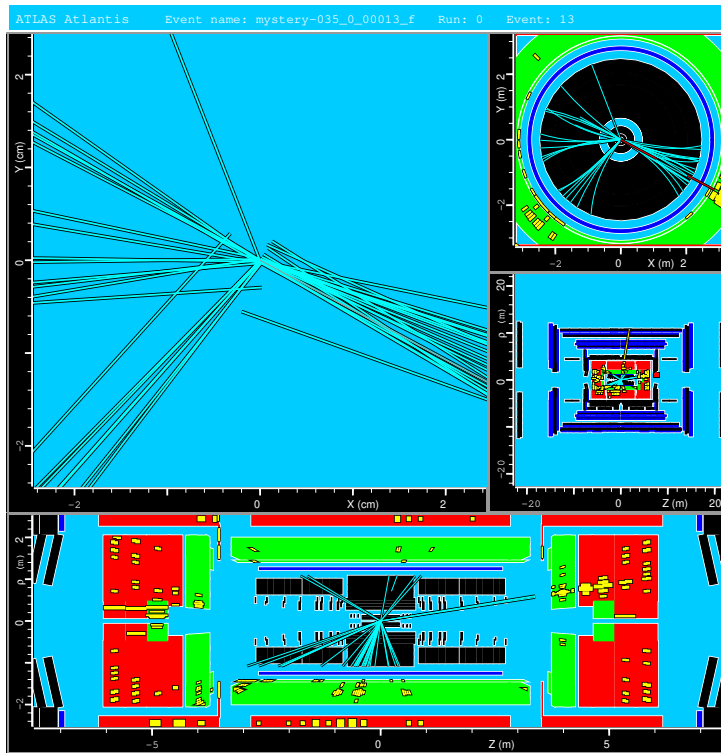
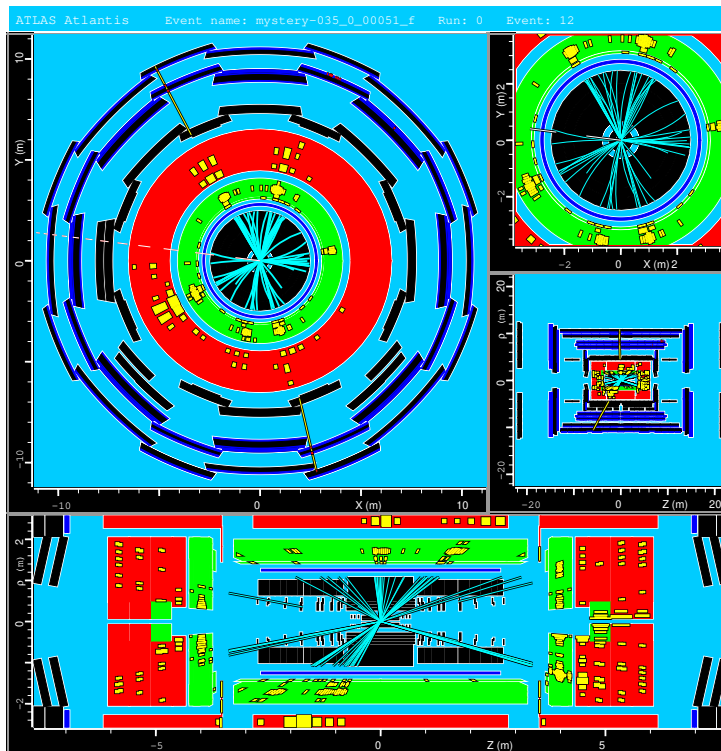Figure 4.1.5: Event name: `mystery-035-f`, Event: 13.



Figure 4.1.6: Event name: `mystery-035-f`, Event: 12.

### 4.1.5 Assignment 8: Cosmic Ray Dataset

In this part of the assignment, we investigated the angular distribution of muons originating from pion decay from air showers in the atmosphere that are detected from the muon chambers in the ATLAS detector. Real ATLAS data from 2007 and 2008 was used in this assignment, contained in the provided file `ATLASData-Cosmics-M5.zip`.

Fig. shows an example of an event observed with this dataset. Note that we have chosen different projections as compared to the figures shown in Sec. 4.1.4 as the projections in such previous figures do not provide any new information in this assignment. We observe that no signatures have been observed in the inner detector as well as in both ECAL and HCAL. This is expected as these muons have momentum of the order of 1 GeV, and as such they do not emit bremsstrahlung and thus no showers are formed in the calorimeters.
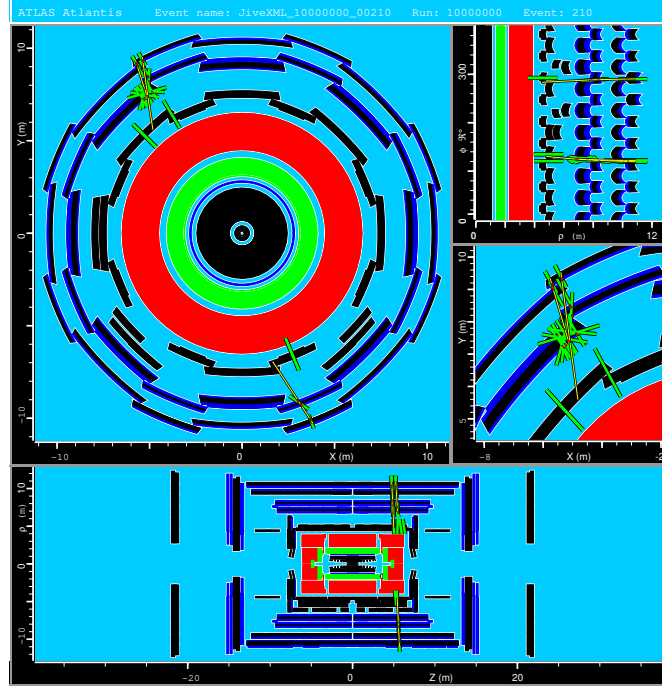


Figure 4.1.7: An example event for cosmic ray muons (Event 210). The reconstructed muon tracks are shown in yellow.

To determine the angle in which the muon has entered the detector, we determined the azimuthal angle $\phi_0$ relative to the ATLAS detector. This is obtained by using the "pick" option in the ATLANTIS program to select each muon track in each event in this dataset. The azimuthal angle was then converted into the zenith angle, i.e. the angle from the local zenith. As $\phi_0 \in [0, 2\pi]$ where $\phi_0 = 0$ is at the positive x-axis, and $\theta \in [-\pi, \pi]$ where $\theta = 0$ is at the local zenith, an azimuthal angle of $\phi_0 = \pi/2$. will be equivalent to $\theta = 0$ as the local zenith is parallel to the y-axis in the detector. Following this logic, we can derive the transformation between $\phi_0$ and $\theta$ as such:

$$\theta = \begin{cases} \phi_0 - \frac{\pi}{2} - & : \phi_0 < \frac{3\pi}{2} \\ (\phi_0 - \frac{\pi}{2}) - 2\pi & : \phi_0 > \frac{3\pi}{2}. \end{cases} \tag{4.1.1}$$

See Appendix A for a more detailed schematic of the transformation.

Fig. 4.1.8 shows the corresponding angular distribution from the cosmic ray muons observed in this dataset, along with the expected distribution $\cos^2(\theta)$ at sea level. Note that we only plot from -90° to 90° as muons produced from beyond the horizon originate from air showers with an extremely low probability.

We observe that while the muon intensity decrease with larger zenith angle, the distribution does not follow a $\cos^2(\theta)$ distribution. This can be attributed to several reasons. Firstly, the ATLAS detector is located 100m below ground, and as such the muons with higher incoming angle will be stopped more by the underground material as compared to those near the zenith. Further, as there are two access shafts located above the ATLAS detector, muons with higher incoming angles interact less with underground
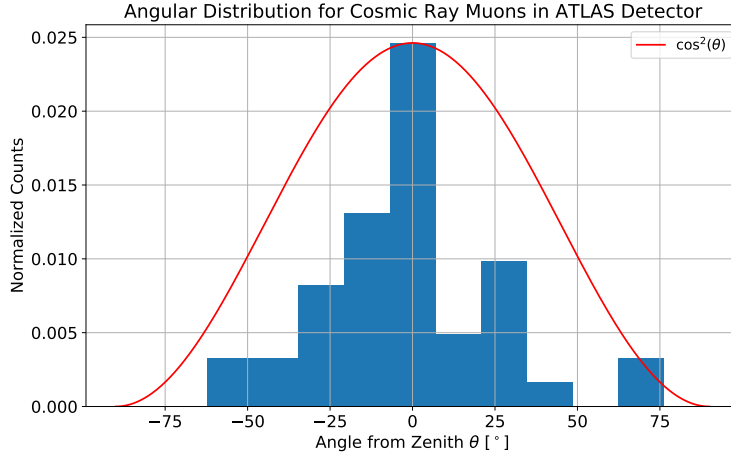
Figure 4.1.8: Angular distribution of cosmic ray muons observed from the ATLAS detector in 2007 and 2008. The expected $\cos^2(\theta)$ is also shown.

material [10]. As such the distribution behaves like $\cos^n(\theta)$ with the exponent $n > 2$. Another reason for this is due to the low statistics, as the the total number of events is $N_{ev} = 65$. With more events, the histogram will be smoother and thus will be able to discern whether the distribution behaves as $\cos^2(\theta)$ or not.

## 4.2    Part 2: Calibration of Electrons

Before performing the measurement of the $W$ mass, the data needs to be calibrated. In this experiment, the raw data was supplied to us and we first have to improve its quality. The most accurate way to determine the energy of electrons is by measuring the deposit in the ECAL. There are several reasons for calibration:

1. The detector consists of hundreds of modules, which will return unequal energy.

2. There could be several parts of the calorimeter which might be inactive.

3. The electron loses a part of its energy in the silicon tracking region before depositing its energy in the calorimeter.

For these reasons, the raw energy values are lower than the true value. Calibration is the way to fix that.

The mass of the $Z^0$ boson is a well known parameter of the SM. It has been measured to a precision of $2 \times 10^{-6}$ relative uncertainty. The width has been measured upto 1 per thousand. Further, we know that most of the electron-positron pairs in an event originate from $Z^0$. Hence, the $Z^0$ peak, which is a well known signal, can be used in order to calibrate our data.

To perform this calibration, we use the library `fitZee.C`, which takes the calibration from the file `ElecCalib.C` and applies that to the data. Applying changes to the `ElecCalib.C` file and compiling `fitZee.C` also changes the `z.Fit()` command. After activating `root`, the following commands are run:

```
.L fitZee.C+
fitZee z
z.Fit("")
```

This creates a calibration object "z" which will be used to calibration. The `z.Fit("")` command fills the histogram and applies the best fit and outputs the fit parameters. The output of this command is shown in Fig. 4.2.1. The $Z$ mass for the uncalibrated data is found to be $89.87 \pm 0.02$ and resolution is $2.588 \pm 0.026$. In the calibration process, the aim is to get the mass as close as possible to the ideal value, which is $91.1876 \pm 0.0021 \mathrm{GeV}/c^2$. Further, the resolution should also be decreased by at least 0.2, while trying to get a good $\chi^2/ndf$ value (ndf stands for number of degrees of freedom). A value
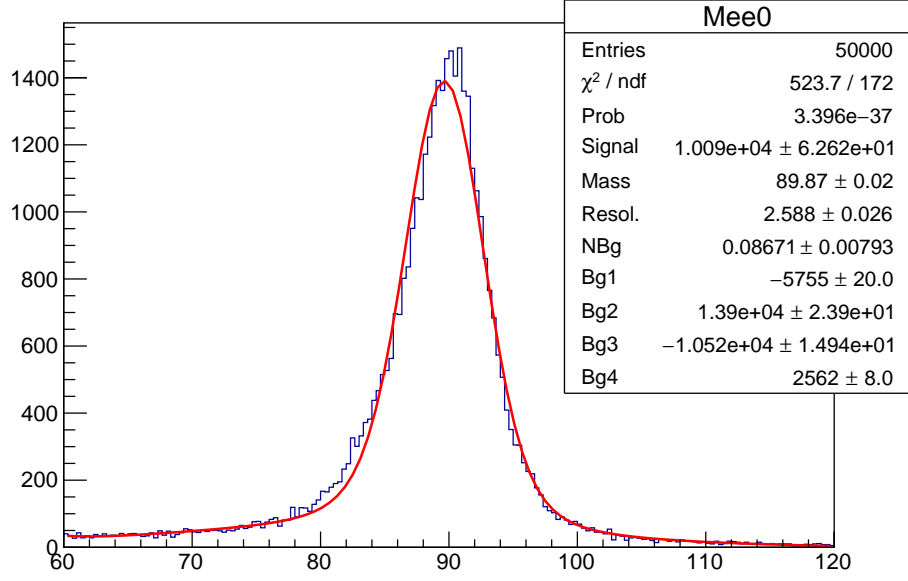
Figure 4.2.1: The output of the uncalibrated data. A resonance near the $Z$ mass can be seen. The red line is the fit and the legend contains the fit parameters.

of approximately 1 is ideal. $\chi^2$ characterizes the characterizes the fit quality and the aim is to usually minimize it. Therefore, a high $\chi^2$ signifies a bad fit.

One can also look at fits with cuts, i.e., looking at how the fit changes for different regions of the parameter spectrum. For instance, to look at the fit in the different regions of the azimutal angle $\phi$, the following command can be run

```
z.Fit("el_phi>0. && el_phi<0.4")
```

Thus, passing the cuts in the fit command allows us to probe different regions of the parameters. The some of the available variables are `el_pt` (transverse momentum of electron), `el_eta` (psuedorapidity), `el_energy` and several others. After applying cuts in several ranges, one can run `z.List()` and looking at the numbers corresponding to different ranges, stack them in the single plot by running

```
z.Draw(0, 1, 2, 3)
```
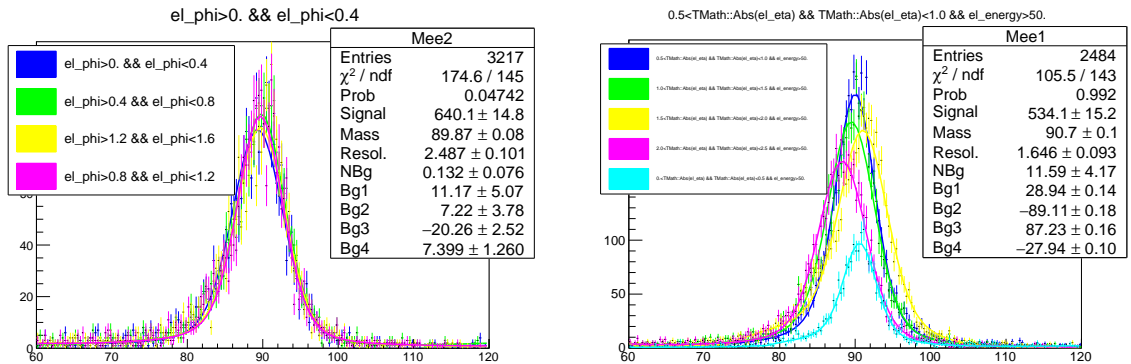


(a) Stacked reconstructed fits of different azimuthal angle, $\phi$, regions.



(b) Stacked reconstructed fits of different pseudorapidity, $|\eta|$, regions.

Figure 4.2.2: Stacked plots of different parameters in different regions. We notice a shift in the peak for different regions.

An example of this is shown in Fig. 4.2.2. A shift in the peak can be seen for different regions. These regions must be studied and calibration must be applied to them. After applying the calibration for several regions, the output is observed and the process is repeated for several more regions and variables. After several trail and errors, we were able to get the desired calibration.

After applying cuts for different regions of a single variable, the calibration was applied and the output was looked at. Then, with this applied calibration, different regions of another variable were compared as mentioned above and the calibration file was modified to correct for this variables. This was done for these set of variables in the following order: phi, eta, mindrjet (which is the minimum distance of the electron to the nearest jet in the $\eta\phi$ plane), etiso (transverse energy of the electron in the area surrounding it in the calorimeter) and pt (transverse momentum). The corresponding plots are shown in Fig. 4.2.3 and the final calibration plot is shown in Fig. 4.2.4. The corresponding code can be found in the Appendix B.
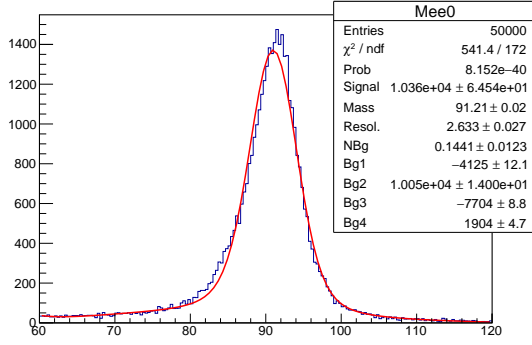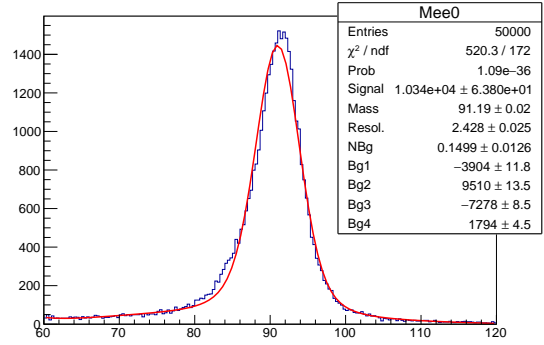


(a) Calibration for only different regions of $\phi$.
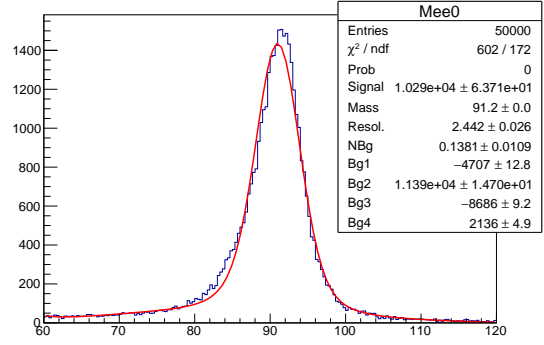
(b) Calibration for $\phi$ followed by $|\eta|$.
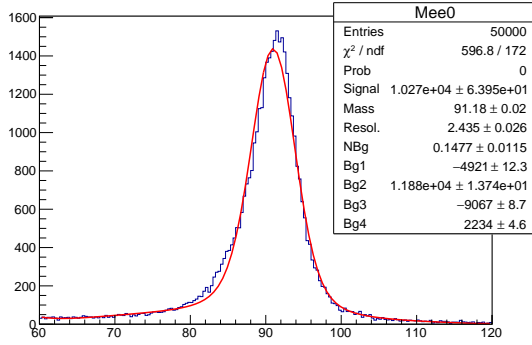
(c) Calibration for $\phi$ and $|\eta|$ followed by mindrjet.

(d) Calibration for $\phi$, $|\eta|$, mindrjet followed by etiso.

Figure 4.2.3: Calibration applied one after the other for different set of variables.

Thus, we were able to get the mass to be $91.198 \pm 0.0196$ and the resolution to be $2.342 \pm 0.024$. $\chi^2/ndf$ is found to be $464.6/172 \approx 2.7$. Using the command `z.Compare()`, we can see the effect of calibration on the data, in Fig. 4.2.5. Further, we also notice a change in the values of mass, resolution and $\chi^2/ndf$. This is because the `Compare()` function uses the "LARGE" argument in the Fit() function, which uses all the data. By running `z.Fit("","LARGE")`, the change in the values was confirmed.
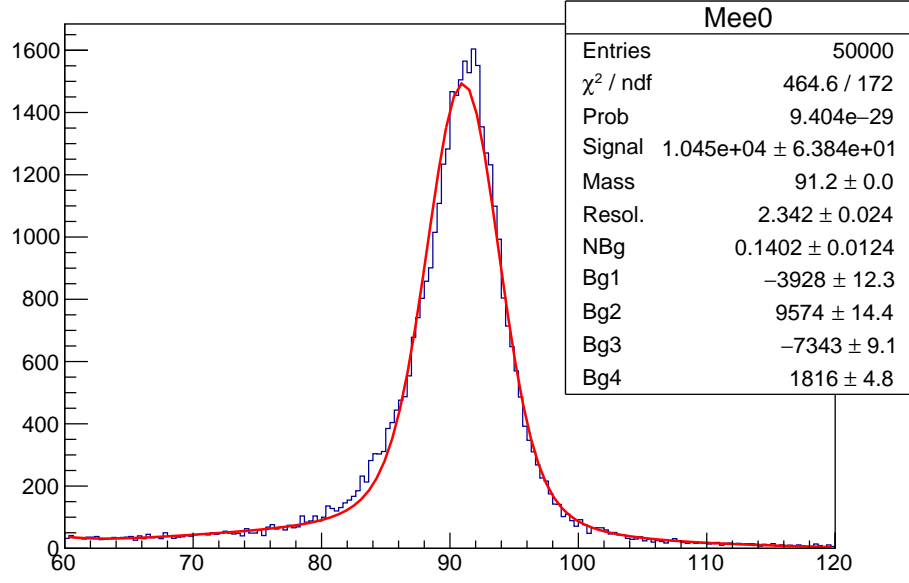
| Mee0 | |
| --- | --- |
| Entries | 50000 |
| $\chi^2$ / ndf | 464.6 / 172 |
| Prob | 9.404e−29 |
| Signal | 1.045e+04 ± 6.384e+01 |
| Mass | 91.2 ± 0.0 |
| Resol. | 2.342 ± 0.024 |
| NBg | 0.1402 ± 0.0124 |
| Bg1 | −3928 ± 12.3 |
| Bg2 | 9574 ± 14.4 |
| Bg3 | −7343 ± 9.1 |
| Bg4 | 1816 ± 4.8 |

Figure 4.2.4: The final fit curve after applying $\phi$, $|\eta|$, mindrjet, etiso followed by $p_T$ calibrations.



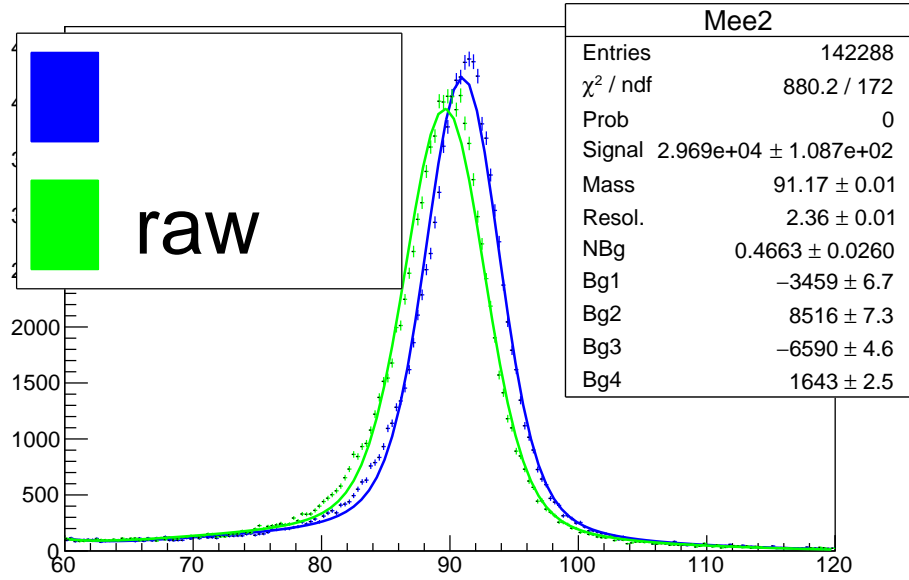| Mee2 | |
| --- | --- |
| Entries | 142288 |
| $\chi^2$ / ndf | 880.2 / 172 |
| Prob | 0 |
| Signal | 2.969e+04 ± 1.087e+02 |
| Mass | 91.17 ± 0.01 |
| Resol. | 2.36 ± 0.01 |
| NBg | 0.4663 ± 0.0260 |
| Bg1 | −3459 ± 6.7 |
| Bg2 | 8516 ± 7.3 |
| Bg3 | −6590 ± 4.6 |
| Bg4 | 1643 ± 2.5 |

Figure 4.2.5: Comparison between calibrated and uncalibrated data. The blue fit corresponds to calibrated data and the green to the uncalibrated data.

# Bibliography

[1] P106: Advanced Laboratory Course, *E214 - The ATLAS Experiment, student manual*, Feb. 2018.

[2] P. A. Zyla *et al.*, "Review of Particle Physics," *PTEP*, vol. 2020, no. 8, p. 083C01, 2020. DOI: 10.1093/ptep/ptaa104.

[3] W. Commons, *File:standard model of elementary particles.svg — wikimedia commons, the free media repository*, [Online; accessed 20-June-2022], 2022. [Online]. Available: https://commons.wikimedia.org/w/index.php?title=File:Standard_Model_of_Elementary_Particles.svg&oldid=652752075.

[4] S. Schael *et al.*, "Precision electroweak measurements on the $Z$ resonance," *Phys. Rept.*, vol. 427, pp. 257–454, 2006. DOI: 10.1016/j.physrep.2005.12.006. arXiv: hep-ex/0509008.

[5] T. Aaltonen *et al.*, "High-precision measurement of the W boson mass with the CDF II detector," *Science*, vol. 376, no. 6589, pp. 170–176, 2022. DOI: 10.1126/science.abk1781.

[6] M. Tanabashi, K. Hagiwara, K. Hikasa, *et al.*, "Review of particle physics," *Phys. Rev. D*, vol. 98, p. 030 001, 3 Aug. 2018. DOI: 10.1103/PhysRevD.98.030001. [Online]. Available: https://link.aps.org/doi/10.1103/PhysRevD.98.030001.

[7] M. W. Krasny, F. Dydak, F. Fayette, W. Placzek, and A. Siodmok, "$\Delta M_W \leq 10 MeV/c^2$ at the LHC: a forlorn hope?" *Eur. Phys. J. C*, vol. 69, pp. 379–397, 2010. DOI: 10.1140/epjc/s10052-010-1417-0. arXiv: 1004.2597 [hep-ex].

[8] G. Aad *et al.*, "Measurements of the Higgs boson inclusive and differential fiducial cross sections in the $4\ell$ decay channel at $\sqrt{s} = 13$ TeV," *Eur. Phys. J. C*, vol. 80, no. 10, p. 942, 2020. DOI: 10.1140/epjc/s10052-020-8223-0. arXiv: 2004.03969 [hep-ex].

[9] A. Tumasyan *et al.*, "Precision measurement of the W boson decay branching fractions in proton-proton collisions at $\sqrt{s} = 13$ TeV," *Phys. Rev. D*, vol. 105, no. 7, p. 072 008, 2022. DOI: 10.1103/PhysRevD.105.072008. arXiv: 2201.07861 [hep-ex].

[10] G. Aad, B. Abbott, J. Abdallah, *et al.*, "Studies of the performance of the ATLAS detector using cosmic-ray muons," *The European Physical Journal C*, vol. 71, no. 3, Mar. 2011. DOI: 10.1140/epjc/s10052-011-1593-6. [Online]. Available: https://doi.org/10.1140%2Fepjc%2Fs10052-011-1593-6.

# Appendix A

# Additional Figures

# Appendix B

# Code

The code for the final `ElecCalib.C` file is shown below.

```
double ElecCalib(double e_raw, double pt, double eta,
 double phi, double etiso, double eoverp, double mindrjet)
{
  double dummy=pt*eta*phi*etiso*eoverp*mindrjet;
  double energy = e_raw;

// final fit parameters and taking the mass of Z as 91.18

  // phi cuts
  if(fabs(phi)>0. && fabs(phi)<0.4) energy = energy * 91.18/89.69;
  else if(fabs(phi)>0.4 && fabs(phi)<0.8) energy = energy * 91.18/89.91;
  else if(fabs(phi)>0.8 && fabs(phi)<1.2) energy = energy * 91.18/89.85;
  else if(fabs(phi)>1.2 && fabs(phi)<1.6) energy = energy * 91.18/89.95;
  else if(fabs(phi)>1.6 && fabs(phi)<2.0) energy = energy * 91.18/89.88;
  else if(fabs(phi)>2.0 && fabs(phi)<2.4) energy = energy * 91.18/89.77;
  else if(fabs(phi)>2.4 && fabs(phi)<2.8) energy = energy * 91.18/90.01;
  else if(fabs(phi)>2.8 && fabs(phi)<3.2) energy = energy * 91.18/89.64;

  // eta cuts
  if(fabs(eta)>0. && fabs(eta)<0.25) energy = energy * 91.18/91.47;
  else if(abs(eta)>0.25 && fabs(eta)<0.5) energy = energy * 91.18/91.43;
  else if(abs(eta)>0.5 && fabs(eta)<0.75) energy = energy * 91.18/91.28;
  else if(abs(eta)>0.75 && fabs(eta)<1.0) energy = energy * 91.18/90.91;
  else if(abs(eta)>1.0 && fabs(eta)<1.25) energy = energy * 91.18/90.84;
  else if(abs(eta)>1.25 && fabs(eta)<1.5) energy = energy * 91.18/90.87;
  else if(abs(eta)>1.5 && fabs(eta)<2.0) energy = energy * 91.18/92.48;
  else if(abs(eta)>2.0 && fabs(eta)<2.5) energy = energy * 91.18/89.83;

  // mindrjet cuts
  if(mindrjet>0. && mindrjet<1) energy = energy * 91.18/91.44;
  else if(mindrjet>1 && mindrjet<2) energy = energy * 91.18/91.19;
  else if(mindrjet>2 && mindrjet<3) energy = energy * 91.18/91.22;
  else if(mindrjet>3 && mindrjet<4) energy = energy * 91.18/91.13;
  else if(mindrjet>4 && mindrjet<6) energy = energy * 91.18/90.51;
  else if(mindrjet>6) energy = energy * 91.18/91.21;

  // etiso cuts
  if(etiso>-10 && etiso<0) energy = energy * 91.18/91.35;
  else if(etiso>0. && etiso<1) energy = energy * 91.18/91.50;
  else if(etiso>1 && etiso<2) energy = energy * 91.18/91.30;
  else if(etiso>2 && etiso<3) energy = energy * 91.18/91.05;
```

```
    else if(etiso>3 && etiso<4) energy = energy * 91.18/90.62;
    else if(etiso>4 && etiso<5) energy = energy * 91.18/90.34;
    else if(etiso>5) energy = energy * 91.18/89.42;

    // pt cuts
    if (pt > 0. && pt < 20.) energy = energy * 91.18 / 89.21;
    else if (pt > 20. && pt < 25.) energy = energy * 91.18 / 90.28;
    else if (pt > 25. && pt < 30.) energy = energy * 91.18 / 90.25;
    else if (pt > 30. && pt < 35.) energy = energy * 91.18 / 90.58;
    else if (pt > 35. && pt < 40.) energy = energy * 91.18 / 90.67;
    else if (pt > 40. && pt < 42.5) energy = energy * 91.18 / 91.24;
    else if (pt > 42.5 && pt < 45.) energy = energy * 91.18 / 91.48;
    else if (pt > 45. && pt < 47.5) energy = energy * 91.18 / 92.05;
    else if (pt > 47.5 && pt < 50.) energy = energy * 91.18 / 92.45;
    else if (pt > 50. && pt < 52.5) energy = energy * 91.18 / 92.30;
    else if (pt > 52.5 && pt < 55.) energy = energy * 91.18 / 91.95;
    else if (pt > 55. && pt < 57.5) energy = energy * 91.18 / 92.18;
    else if (pt > 57.5 && pt < 60.) energy = energy * 91.18 / 91.95;
    else if (pt > 60. && pt < 65.) energy = energy * 91.18 / 92.00;
    else if (pt > 65. && pt < 70.) energy = energy * 91.18 / 92.05;
    else if (pt > 70. && pt < 75.) energy = energy * 91.18 / 91.88;
    else if (pt > 75. && pt < 80.) energy = energy * 91.18 / 91.77;
    else if (pt > 80. && pt < 100.) energy = energy * 91.18 / 91.74;
    else if (pt > 100. && pt < 150) energy = energy * 91.18 / 91.96;

    return energy;
}
```